



An origami like 3D patterned cellulose-based scaffold for bioengineering cardiovascular applications

Gabriela Melo Rodriguez · Donata Trueb ·
Joachim Köser · Joachim Schoelkopf ·
Maurizio Gullo

Received: 20 October 2022 / Accepted: 1 September 2023 / Published online: 27 September 2023
© The Author(s) 2023

Abstract In this work we describe the manufacturing of cellulosic, cell compatible scaffolds with an inherent 3D origami crease pattern for applications in cardiac tissue engineering. Different cellulosic materials were studied, among them cotton linters, fibers obtained from eucalyptus, pine, spruce and lyocell. Formed sheets made of cotton linters were chosen for further study due to the highest biocompatibility and mechanical properties best suited for cardiomyocytes in wet and dry conditions: E - modulus of 0.8 GPa, tensile strength of 4.7 MPa and tensile strength in wet environment of 2.28 MPa. Cell alignment is desired to achieve directional contraction of the cardiac tissue, and several options were investigated to achieve fiber alignment, e.g. a dynamic sheet former and Rapid Köthen sheet former. Although the orientation was minimal, cells cultured on the cellulose

fibers grew and aligned along the fibers. Origami inspired crease patterns were applied to the cellulose scaffolds in order to introduce directional flexibility beneficial for cardiac contraction. The transfer of a Miura-ori crease pattern was successfully applied in two ways: folding of the dried sheet between PET foils pre-formed in a 3D printed mold, and in situ wet fiber molding on a 3D-patterned mesh mounted in the sheet former's sieve section. The latter approach enables upscaling for potential mass production.

Keywords Cardiac tissue engineering · Cellulose scaffold · Cytocompatibility · Volumetric origami constructs

Introduction

Tissue engineering is a rapidly growing field which aims to produce models for skin, heart, bone and eventually whole organs. In a first approach, the creation of tissue models for pharmacological research is envisioned, with a view to substantially reducing animal trials. Recent progress in biofabrication has enabled the manufacturing of 3D tissue models through layer by layer deposition of cell-laden hydrogel onto scaffolds acting as cell culture support structures (Moroni et al. 2018).

Similarly, paper-based cell culture supports have been used for tissue engineering (Chen et al. 2015; Juvonen et al. 2013; Ng et al. 2017; Park et al. 2014)

G. M. Rodriguez (✉) · J. Schoelkopf
New Application Research, Omya International AG,
4622 Egerkingen, CH, Switzerland
e-mail: gabriela.melorodriguez@omya.com

D. Trueb · M. Gullo
School of Life Sciences, Institute for Medical Engineering
& Medical Informatics, University of Applied Sciences
and Arts Northwestern Switzerland, 4132 Muttenz, CH,
Switzerland

J. Köser
School of Life Sciences, Institute for Chemistry
and Bioanalytics, University of Applied Sciences and Arts
Northwestern Switzerland, 4132 Muttenz, CH, Switzerland

due to their capacity to wick liquids by capillarity, their porous matrix enabling the transport of nutrients and oxygen (Chen et al. 2015; Deka et al. 2020), as well as the availability of cell migration paths along the fibers (Mosadegh et al. 2014, 2015; Ng et al. 2017; Wang et al. 2015). Furthermore, paper scaffolds are foldable, mechanically flexible, easy to sterilize (Lantigua et al. 2017) and can be produced in large quantities at low cost (Juvonen et al. 2013) compared to materials such as polymers, glass and metals (Juvonen et al. 2013; Lantigua et al. 2017). Different cellulosic materials have been used for paper based scaffolds (Lantigua et al. 2017), for example, print paper from wood pulp has been used by Wang et al. to support beating cardiac tissue (Wang et al. 2015), cotton fibers have been employed to support cells from tissues such as cardiomyocytes, human breast cancer and other human cells (Ng et al. 2017) and lyocell has been used as a scaffold for cartilage tissue engineering (Müller et al. 2006). Recently, cellulose based paper has been used as a support in biofabrication (Ng et al. 2017) such as bioprinting (Derda et al. 2011; Lantigua et al. 2017; Mosadegh et al. 2014; Ng et al. 2017; Wang et al. 2015).

A desired feature of cell culture scaffolds is the availability of alignment cues, both to guide and promote cell maturation (Parrag et al. 2012; Wanjare et al. 2017). Alignment cues for neuronal cell cultures have been achieved by several techniques such as electrospinning (Rayatpisheh et al. 2014; Tseng et al. 2013; Whited and Rylander 2014) or casting hydrogels onto molds containing nanometer sized grooves (Tsai et al. 2017). Similarly, anisotropic alignment structures for cardiac cell cultures act as guides for directional muscle fiber growth and differentiation, resulting in directional and higher overall contraction forces (Kharaziha et al. 2013; Radisic et al. 2004; Wanjare et al. 2017). Cellulose fibers with a specific diameter might also function as alignment cues. Cell culture paper scaffolds with such intrinsic alignment cues would not require post fabrication steps and could thus easily mass be produced. However, almost all paper sheets made at lab, pilot and industrial scale have a mandatory fiber alignment given by the machine direction (MD) and the cross direction (CD) related forces involved in the elaboration process (Belle and Odermatt 2016; Kröling et al. 2014). To achieve cellulose cell culture scaffolds with oriented

fibers and tailored fiber diameters, current fabrication procedures need to be adapted.

Successful cell differentiation and maturation often depend on the mechanical characteristics of the supporting cell scaffold (Moroni et al. 2018). By introducing crease patterns, the directional elongation potential and cross lateral stability of paper scaffolds can be adapted to match the desired tissue properties. Origami techniques have been used to introduce tailored mechanical properties in cellulose scaffolds for engineered tissue (Li et al. 2020), drug delivery and catheters (Ahmed et al. 2020). Additional benefits of using origami techniques are the low material costs, scalability, versatility and the possibility to fold planar origami substrates into complex volumetric structures (Dudte et al. 2016; Kuribayashi et al. 2006; Li et al. 2017; Rodrigues et al. 2017; Woodruff and Filipov 2021, 2022) such as heart ventricles (Ahmed et al. 2020). Cellulose scaffold manufacturing techniques able to introduce origami crease pattern in a cost-effective manner would therefore be desirable.

This work aims to realize current cellulose based cell culture scaffolds suitable for a wide range of tissues. It focuses on the cost-effective manufacturing of biocompatible and cell culture resistant cellulose scaffolds with fiber dimensions enabling aligned cell growth, fiber alignment for directionally tailored mechanical properties as well as in-process formation of origami crease patterns. This research is part of a larger project whose objective is the combination of cellulose scaffolds with layers of cardiac and vascular forming cells, enabling the engineering of cardiac tissue for miniaturized heart models and cardiac patches for regenerative surgery.

Materials and methods

The fiber materials listed in Table 1 were used to produce the cellulose scaffolds. The cellulose used in this study came from bleached kraft pulps, the process can contain NaOH, O₂, NaClO₃, EDTA, SO₂, H₂O₂, O₃, MgSO₄, CaO, Cd, Pb, Cu, Cr, Ni, Zn, suggesting that fibers can also contain traces of them. The biocompatibility and mechanical properties of the scaffolds were assessed to understand the role of cellulose in the final construct. The elaboration and procedures performed on the paper are described below.

Table 1 Cellulose fiber material composition and fiber dimensions

Sample N°	Cellulose fiber composition	Fiber width (μm)	Fiber length (mm)	Measured method provided by supplier	Supplier
1	Eucalyptus 100%	12	0.9	Fiber image analyzerFS5	Fibria
2	Pine 20–30%, spruce 70–80% (NBSK)	30	2.4–2.6	Kajaani MAP	Mercer Pulp
3	Lodgepole pine 50–60%, White spruce 30–40%, sub-alpine fir 5–10% (NBSK) Other 0–10%	28–29	2.51	Kajaani FS200	Canfor
4	Pine 70–100%, spruce 0–30%	23.75	1.8	Kajaani FSA	Metsä
5	Cotton linters 100%	18 ± 6.2	3 ± 0.9	Length stereo microscope reflected light ring light, width transmitted light brightfield*	Research purpose
6	10 wt % Lyocell fiber produced by a solvent spinning process. Raw material used is wood pulp derived from eucalyptus, pine and beech trees. 90 wt % Sample 2	12	10	Controlled process	Lenzing

*Measurements performed under optical inspection in 10 samples

Paper elaboration

Papers were mainly produced using a Rapid Köthen sheet former from Gerd Senkel and a dynamic sheet former (DSF) from CanPa. The Rapid Köthen system triggers a typical stochastic distribution of the fibers in normal use, whereas the DSF can be employed to induce fiber alignment by means of a rotational mesh in the form of a cylinder. For both methods paper sheets of 40 g m^{-2} were produced. Conditions for each method are described below.

Rapid Köthen sheet former

ISO 5269-2 norm was employed for paper sheet production. Waterborne diluted fibers (40 g L^{-1}) were suspended in a cylindrical vessel and filled with water to the final volume of 6 L. The fibers were agitated using air-bubbling through the vessel for 5s followed by dewatering by vacuum. The fibers were distributed on the bottom of the apparatus and collected by a metallic wire mesh (bronze top mesh supported by steel grid) into a wet mat, then transferred to a carrier board for further dewatering and drying.

Dynamic sheet former

A suspension of 0.23 wt% of solid content made up of fibers and water was sprayed with a flow rate of 9.9 L min^{-1} on a rotatory cylindrical mesh with a speed of 1400 min^{-1} . The excess water was removed by centrifugal forces. The formed sheet was transferred to a carrier board where the wire was removed and the sheet was dewatered twice using pressure, and dried in a drum drier at $60 \text{ }^\circ\text{C}$.

Origami design and 3D pattern transfer

Other features such as patterning can be added to the scaffolds without modifying the porosity and structure of the paper. Some of the most common origami crease patterns use for tessellation are Yoshimura pattern, diagonal pattern, waterbomb base and Miura-ori pattern (Parnell 2021). For this study the Miura-ori origami fold pattern was applied to the paper, with the aim of increasing the freedom of contraction and stretching without unwanted warping. As shown in Fig. 1, the Miura-ori origami pattern is based on the tessellation of flat parallelograms which are mirror reflected along the parallel direction and translated along the perpendicular direction, alternating

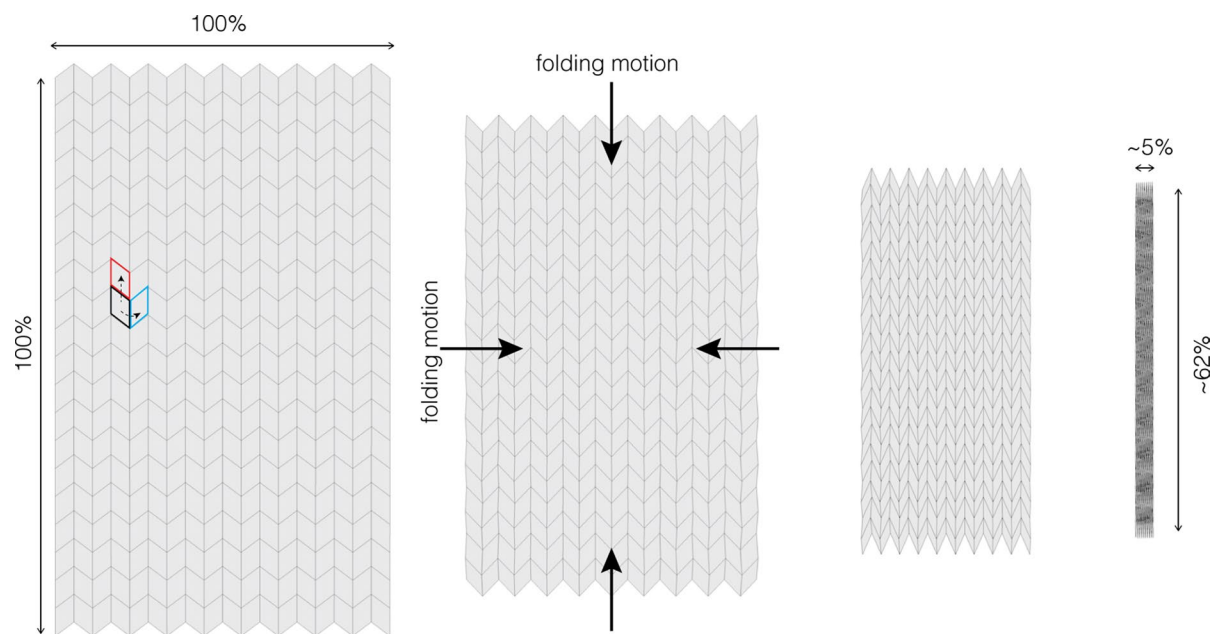


Fig. 1 Schematic representation of Miura-ori origami pattern generated by the translation (red) and reflection (blue) of a rhombus. Longitudinal contraction of the Miura-ori pattern will lead to an axial contraction

between mountain and valley folds (Miura 1985; Reid et al. 2017; Schenk et al. 2011; Schenk and Guest 2013). The contraction of the origami along the longitudinal direction will lead to a contraction along the axial direction (Fig. 1).

The Miura-ori pattern therefore has a negative Poisson's ratio as well as an anisotropic contraction ratio (lateral vs. longitudinal). These characteristics are key when engineering scaffolds for tissue engineering, in particular for cardiac tissue which contracts in all directions when moving (Kim et al. 2021). To further accentuate the contraction in one direction, the parallelogram side lengths were 300 μm , 250 μm and angles were 35°, 55° respectively. This resulted in an auxetic structure with Poisson's ratio of $\nu = -0,65$ with an anisotropic contraction ratio of 2.5 which is in the range most appropriate for cardiac tissue (Kapnisi et al. 2018). For proof of principle only one pattern was fabricated and assessed. However, all parallelogram dimensions and shapes can be used as the basis for a Miura-ori pattern scaffold for cardiac tissue engineering when satisfying a negative Poisson's ratio and anisotropic contraction ratio between 1,9 and 3.9 (Kapnisi et al. 2018).

First prototypes of folded scaffolds were manufactured by dry embossing (Method A, Fig. 2). In view

of future mass production of origami scaffolds, a second more scalable approach for origami transfer was developed (Method B, Fig. 2). In both cases the templates contained the origami pattern with 30° fold angle.

Finally, the papers produced by either of the methods were stabilized by mounting them in a further 3D printed origami shape, wetted with gelatin hydrogel and enzymatically crosslinked in a cell culture incubator. The origami scaffolds were then conserved in wet conditions in sterile filtered phosphate buffered saline solution for several weeks without degradation or dissolution. The two methods, to generate the 3D origami crease pattern on the paper, before mentioned are explained as followed and schematically represented on Fig. 2.

Method A, dry embossing

Two 75 μm thick PET foils were thermoplastically deformed ($T=80\text{ }^{\circ}\text{C}$, $P=100\text{ g cm}^{-2}$, $t=1\text{ h}$) into the Miura-ori pattern, by pressing between two previously 3D printed stamps (Formlabs, DentalSG) Fig. 3. The paper was sandwiched between the two Miura-ori patterned PET preforms and the sandwich was folded and unfolded until the desired pattern was

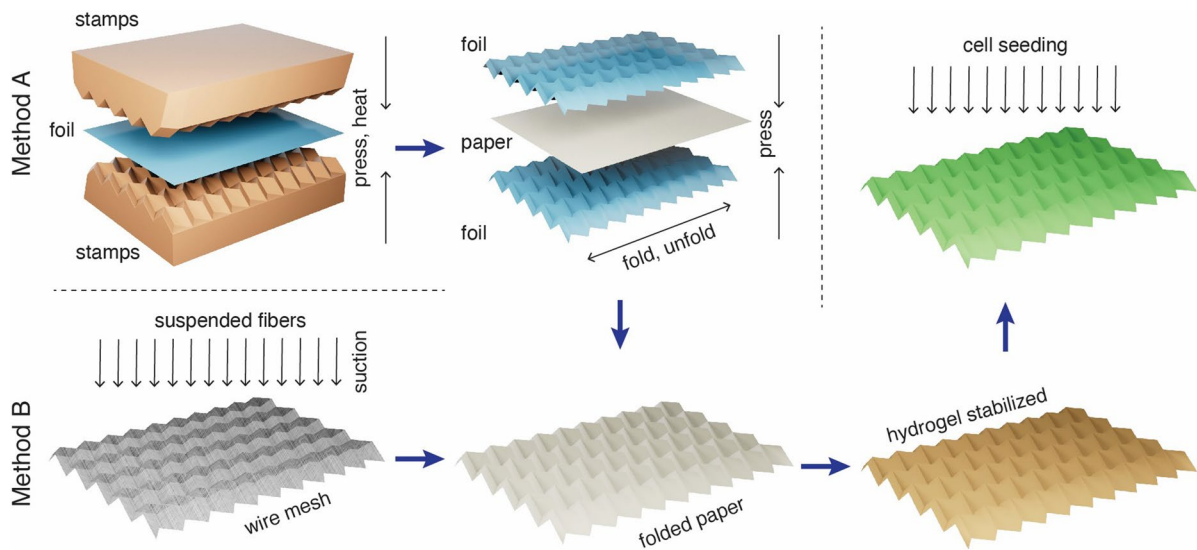


Fig. 2 Schematic depiction of the two Origami pattern transfer methods used. Method A, dry embossing: The pattern is first transferred to a pair of plastic foils by hot embossing. The foils are used to transfer the origami pattern onto a cellulose sheet by pressure and constant folding and unfolding; Method

B, wet transfer: the origami pattern is generated directly during paper formation onto a wire mesh containing the crease pattern. The wire mesh was either formed by embossing a planar wire mesh, similar to the foils in method A or was directly 3D printed

reached on the paper (Fig. 3b). The foils could be used several times. The folding and unfolding of the foil-paper-foil sandwich allowed the paper to slide into place during the folding process without tearing, as would have been the case if embossing with rigid stamps. To avoid tearing or thinning of the paper scaffolds during embossing, a dynamic 2 step pattern transfer similar to that used in the textile industry was adapted (Philpott 2012).

Method B: wet forming

The origami pattern was generated in situ during the wet paper forming process on a wire mesh containing the origami crease pattern in the sheet former's draining section. Two approaches were used to produce the patterned wire mesh: the first variant employed a 3D printed origami shaped mesh (DentalSG, Formlabs) mounted on a standard wire mesh (Fig. 3c); In the second approach the 3D pattern was embossed into a standard wire mesh using 3D patterned stamps similar to the one used in method A (Fig. 3e). The sieved paper was dried on the modified mesh in the oven for 15 min at 120 °C. Thereafter, the patterned paper was removed from the wire mesh (Fig. 3f).

Stabilization of the cellulose scaffold

To guarantee the structural stability of the cellulose scaffolds when kept in culture media for a prolonged time, they were fixed by the addition of hydrogel. The addition of hydrogel served two purposes, stabilize the cellulose paper in for long term cell culture and avoid its disassembling in single fibers. The folded scaffolds were therefore mounted on a 3D printed form with the same origami pattern and impregnated with 20 μ l of 10%w/v gelatin (Porcine skin, Sigma Aldrich) solution including 1% v/v transglutaminase enzyme. The amount of the hydrogel in the papers was controlled by pipetting a specific volume of hydrogel to the paper such that the paper is not wetted until the borders, condition needed for posterior manipulation of the scaffold. This ensured the full adsorption of the hydrogel into the scaffold. The assembly was allowed to enzymatically crosslink in a conventional cell culture incubator at 37 °C 5% CO₂ and 95% RH for 30 min. In addition, the hydrogel wetted paper was sandwiched/pressed between two polymeric foils during origami folding and crosslinking, which further distributed and promoted the hydrogel absorption.

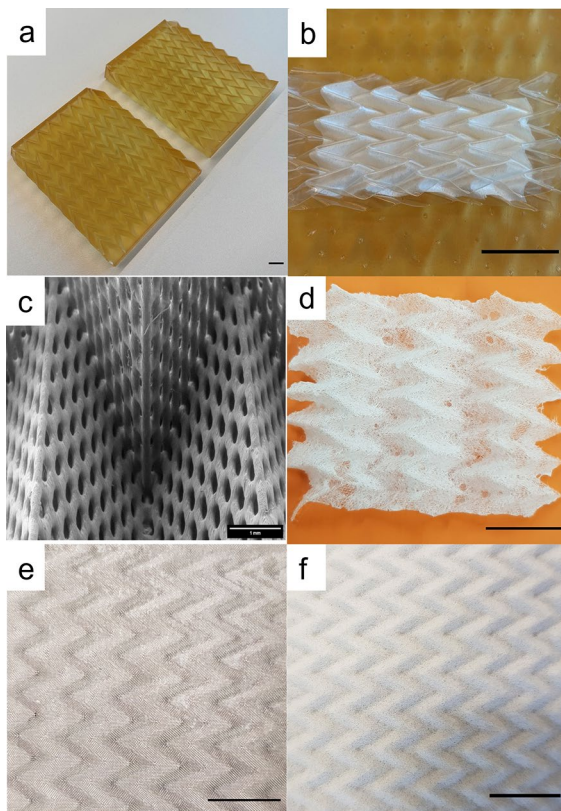


Fig. 3 Origami patterns on paper scaffolds **a** 3D printed Origami stamps; **b** pattern transfer by deforming the pair of origami foils enclosing the paper scaffold; **c** SEM picture of 3D printed polymer sieve; **d** fibers on polymer sieve; **e** preformed metallic mesh; **f** paper with 3D origami shape after demounting from the preformed origami mesh (Scale bars 1 cm when not mentioned)

Mechanical properties of papers

Dry papers

The mechanical properties in MD and CD were first evaluated for the dry and un-stabilized papers. All samples were measured under controlled conditions (50% RH and 23 °C) according to ISO 187. The mass was measured using an analytical balance according to ISO 536. The thickness of the papers was measured with a Lorentzen & Wettre micrometer according to EN ISO 12625-3. The specimen dimensions for the samples elaborated with the Rapid Köthen and DSF were 15 mm wide × 150 mm long (clamping length 100 mm). For each measurement 10 specimens were evaluated in a Lorentzen & Wettre tensile tester

using a speed of 10 mm min⁻¹ for the tensile test. DSF sheets were evaluated in MD and CD while the samples produced with the Rapid Köthen were evaluated in random directions.

Wet papers

The mechanical properties of stabilized papers were assessed in wet conditions. For each material five wetted specimens were measured under the same room and machine conditions and specimen size described above. Tensile strength was calculated from the measured data (tensile force/initial width of the specimen).

Confocal micrographs and fiber alignment analysis

Six confocal images of sheet papers were taken with 1536 × 1536 pixels/image, (array of 6 × 6 images with a resolution of 256 × 256 pixels). Magnification of 200 ×. Highpass filters with a threshold of 250 μm were applied.

Cell Culture

Cytocompatibility assays were performed using rat2 fibroblasts (ATCC CRL-1764). Cells were grown in complete growth medium (DMEM + 10% FCS + penicillin-streptomycin) and seeded onto stabilized cellulose paper samples. Before reaching confluency, typically after 2 days, cytocompatibility was assessed by a metabolic assay applying resazurin (see following section).

Cytocompatibility studies

A Resazurin stock solution of 4 mg ml⁻¹ was diluted 1:1000 in serum free culture medium. The solution was then added to the cell cultures and incubated for 8 h in the incubator prior to measurement. Reference cells were cultured on standard cell culture plastic and viability was assessed by quantifying the fluorescence intensity and comparing it to the reference. Samples with values near to the reference were considered to have good cell viability for the purpose and promising cytocompatibility. For visual examination, cells cultured on paper samples were stained with a mixture of syto 9 (Thermo Fisher Scientific) and propidium iodide (Thermo Fisher Scientific) which

allows discrimination of dead (red) and live (green) cells by fluorescence microscopy.

Results and discussions

Mechanical properties of papers with anisotropic fiber orientation produced with Rapid Köthen sheet former

Papers with random fiber alignment produced by the Rapid Köthen sheet former were tested first. To assess the basic mechanical properties of the different materials, the cellulosic paper sheets were first tested in dry conditions. Table 2 shows the values of strain at break, tensile strength and E- Modulus for each of the paper sheets assessed.

The wide range of breaking strength (1–2.3%), tensile strength (4.7–35 MPa) values and the high E-modulus (0.8–4.4 GPa) demonstrates the versatility of cellulosic material to structurally support fragile cell hydrogel cultures. In cardiac tissue engineering the materials reported are commonly hydrogels with an E-modulus around 6.7 MPa (Eslami et al. 2014), tensile strength range between 6 and 23 MPa (Pushp et al. 2021) and strain at break of ca. 200% (Hidalgo-Bastida et al. 2007; Pushp et al. 2021). The tensile stresses of the cellulose papers and cardiac tissue compare well, which is an important factor for promoting cardiac cell maturation. However, the high E-modulus of the cellulosic papers compared with the cardiac tissue will result in less deformation for plain papers. In this regard the crease pattern may offer an advantage over planar paper sheets. For paper without cardiac cells, the break stress of the cellulosic scaffold is much lower than cardiac tissue. As shown

Table 2 Mechanical properties of elaborated papers (40 g m⁻²) with the Rapid Köthen

Sample N°	Strain at break (%)	Tensile strength(MPa)	E-modulus (Gpa)
1	1.0 ± 0.2	13.4	2.8 ± 0.2
2	1.3 ± 0.2	9.1	1.8 ± 0.2
3	1.8 ± 0.1	20.6	3.4 ± 0.5
4	1.5 ± 0.1	17.9	3.0 ± 0.4
5	1.3 ± 0.1	4.7	0.8 ± 0.1
6	2.3 ± 0.2	35.0	4.4 ± 0.2

below, the break and tensile stress will change in wet conditions. Mixtures of fibers such as in sample 6 (see Table 1) where pine and spruce were blended with lyocell had an increase in the mechanical properties of at least 50% compared with sample 2 without lyocell. This suggests that the mechanical properties of the cellulosic paper can be further tuned to obtain the desired final values. Overall, the use of cellulosic paper as cell culture scaffold may improve the handleability of the final tissue with less deformation and under tissue-comparable stress conditions.

In a second mechanical assessment, the cellulosic scaffolds were tested in wet and stabilized conditions. The tensile strength in wet conditions for the scaffolds with the highest biocompatibility, pine/spruce and cotton linter scaffolds (samples 2 and 5 - see below), was calculated. The values were 3.74 and 2.28 (MPa), respectively. These values are in accordance with the range of hydrogel scaffolds suitable for cardiac tissue engineering, which is around 1.3–3 MPa in a wet environment (Pushp et al. 2021). This suggests that the wet cellulosic papers could work in such an application.

Mechanical properties of papers produced with dynamic sheet former

The directional fiber orientation for cellulosic scaffold sheet can be enhanced by the DSF technique. The homogeneity of fiber orientation can be measured by comparing the tensile strength in MD and CD. Table 3 shows the mechanical properties of MD and CD of cellulosic scaffolds produced by DSF. The tensile strength on MD is almost double compared with CD, which is an indication of substantial fiber alignment. For this part of the study only the fibers with the best biocompatibility (study shown below) were processed by the DSF.

Table 3 Mechanical properties of cotton linter paper elaborated with DSF

Cotton linters fiber, 49.5 g m ⁻² , thickness 111.7 ± 2.1 μm	MD	CD
Strain break (%)	2.29 ± 0.16	2.53 ± 0.16
Tensile strength (MPa)	9.29	5.12
E-Modulus (GPa)	1.52 ± 0.10	0.79 ± 0.02

However, confocal and image analysis of the DSF papers still show a strong degree of random orientation. The distribution of the fibers is shown on the confocal (Fig. 4) giving the topographical details within a layer of 20 μm described in the grey colormap. Both sides of the paper were characterized because one side of the paper was exposed directly to the centrifugal forces of the DSF and it was expected that the fibers were more aligned than the top surface. Although only the fiber orientation of the outer layers on both sides of the scaffolds could be characterized, we assume a similar distribution of the inner structure of the paper scaffolds. It is possible to distinguish that fibers are in all directions and is not a clear pattern of directionality. This is why the idea of using the fibers themselves as orientation templates for the cells has been abandoned (see Fig. 4).

Hydraulic turbulence and interactions between the fibers in the cellulose matrix during the transition from wet to dry form, e.g. hydrogen-bonding, van der Waals interactions and capillary forces, (Wohlert et al. 2021) probably introduce an unavoidable element of stochasticity. In order to have fibers aligned to a degree that can work for cell alignment, other techniques need to be applied.

Cytocompatibility and cell alignment

To assess the cytocompatibility of the cellulose materials, Rat2 fibroblast cells were seeded onto the stabilized scaffolds and cultured for 2 days. Viability of the cells was quantified by a resazurin based metabolic assay. Cells cultures on standard tissue culture plastic dishes were taken as positive control. In parallel, to visualize cell arrangement on the paper samples, dead/live staining was performed for all the samples evaluated in the cytocompatibility study. The graph in Fig. 5 shows good viability of the fibroblast cells on all the fiber materials; cells cultured on cotton linters even showed a superior viability, higher than the positive test. This can be due to the porous structure (as shown in Fig. 4) that allows nutrients and biochemical signals to be transported within the matrix. Cells cultured on pine and lyocell fibers showed a satisfactory viability which can be used as a second material choice. The slight difference of biocompatibility between samples could be attributed to the condition that cellulose fibers taken from processed wood can contain traces of different components.

The fluorescent micrographs (Fig. 6a and b) show the stained cell cores as well as a slight autofluorescence background of the fibers. It is clearly visible that the cells grow preferentially on fiber structures rather than between the fibers. Furthermore, the

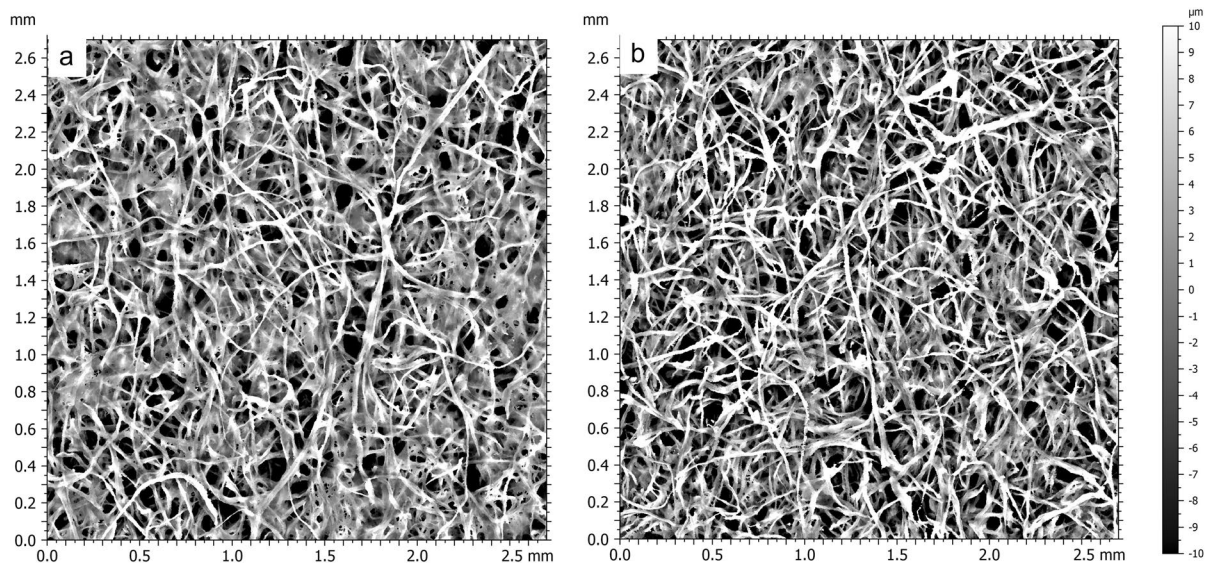


Fig. 4 Confocal images of cotton linters processed on the dynamic sheet former **a** top side of the cellulose paper and **b** bottom side of the cellulose paper (close to the wire)

Fig. 5 Intensity of resorufin fluorescence based metabolic assay for cells grown on different paper samples (Table 1) compared to cells grown on tissue culture plastics (red line)

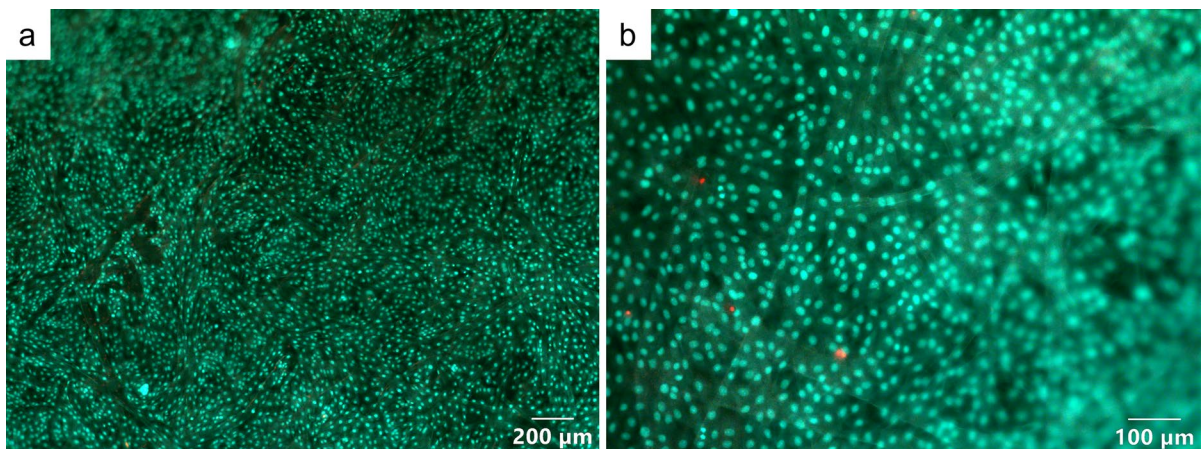
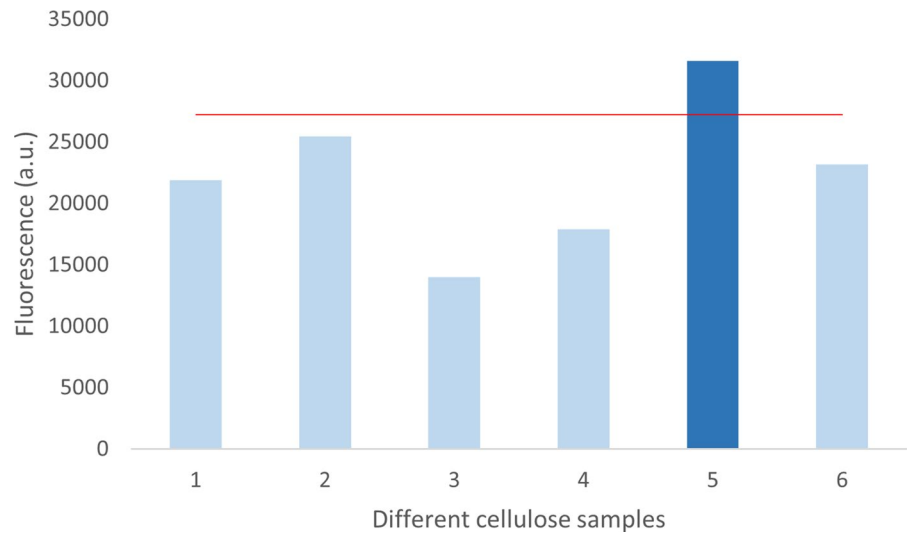


Fig. 6 Fluorescence microscope images of “dead/live” stained rat2 cells aligned on cotton linter fibers, demonstrating the absence of dead cells (red nuclei). Note the frequently

observed linear alignment of cells, presumably along individual cellulose fibers **a** 200 µm scale **b** 100 µm scale

tightly packed equidistant distribution of cell nuclei suggests a high confluency, which in turn supports the preferential cell growth on the fiber’s structures. The few red cell cores depict dead cells and demonstrate the high cytocompatibility of the cellulose scaffold. This suggests that in future, plating cells on cellulose scaffolds with directionally aligned fibers (not the case in this study) might result in tissue scaffolds with directionally aligned cells. In particular for cardiac tissues, this property is of great importance in achieving native anisotropic contraction (Kapnisi et al. 2018). This is also shown in many studies where

fiber alignment potentially enhances cell organization in the direction of the construct (Collinsworth et al. 2000; Kai et al. 2011; Ker et al. 2011; Khan et al. 2015).

Conclusion

Cellulose scaffolds made of cotton linters stabilized with gelatin hydrogel could be used as support cell cultures in tissue engineering thanks to their mechanical properties and biocompatibility. It was also shown

that a combination of different fibers could help to adjust the final desired mechanical properties of scaffolds. For cardiovascular applications, alignment of the cultured cells is generally desired. In this study a degree of fiber alignment (templating cell alignment), was obtained using a dynamic sheet former, but it was not enough for the application mentioned and more work in that direction needs to be done. However, methods have been successfully developed to generate the origami crease pattern on the cellulose scaffold during the paper formation process. This opens up the possibility of producing origami style folded scaffolds facilitating coordinated cell contractions in a 3D spatial configuration.

Acknowledgements The authors greatly acknowledge the support of Dr. Johannes Kritzing for consulting on the fiber selection. The authors greatly acknowledge financial support from the Swiss Nanoscience Institute (SNI) NanoArgovia Project KOKORO (A14.07).

Author contributions GMR, MRG, JS contributed to the study conception design. Material preparation, data collection and analysis were performed by GMR, DT and JK. The first draft of the manuscript was written by GMR, MRG, JS and JK commented on previous versions of the manuscript. All authors* read and approved the final manuscript.

Funding The authors greatly acknowledge financial support from the Swiss Nanoscience Institute (SNI) NanoArgovia Project KOKORO (A14.07).

Data availability All data generated or analyzed during this study are included in this published article.

Declarations

Conflict of interest The authors Gabriela Melo Rodriguez and Joachim Schoelkopf are employees of Omya International AG. In addition, the study was financial supported from the Swiss Nanoscience Institute (SNI) NanoArgovia.

Ethical approval Not applicable.

Consent for publication Not applicable.

Open Access This article is licensed under a Creative Commons Attribution 4.0 International License, which permits use, sharing, adaptation, distribution and reproduction in any medium or format, as long as you give appropriate credit to the original author(s) and the source, provide a link to the Creative Commons licence, and indicate if changes were made. The images or other third party material in this article are included in the article's Creative Commons licence, unless indicated otherwise in a credit line to the material. If material is not included in the article's Creative Commons licence and your

intended use is not permitted by statutory regulation or exceeds the permitted use, you will need to obtain permission directly from the copyright holder. To view a copy of this licence, visit <http://creativecommons.org/licenses/by/4.0/>.

References

- Ahmed AR, Gauntlett OC, Camci-Unal G (2020) Origami-inspired approaches for biomedical applications. *ACS Omega* 6(1):46–54. <https://doi.org/10.1021/acsomega.0c05275>
- Belle J, Odermatt J (2016) Initial wet web strength of paper. *Cellulose* 23(4):2249–2272. <https://doi.org/10.1007/s10570-016-0961-7>
- Chen YH, Kuo ZK, Cheng CM (2015) Paper: a potential platform in pharmaceutical development. *Trends Biotechnol* 33(1):4–9. <https://doi.org/10.1016/j.tibtech.2014.11.004>
- Collinsworth AM, Torgan CE, Nagda SN, Rajalingam RJ, Kraus WE, Truskey GA (2000) Orientation and length of mammalian skeletal myocytes in response to a unidirectional stretch. *Cell Tissue Res* 302(2):243–251. <https://doi.org/10.1007/s004410000224>
- Deka B, Kalita R, Bhatia D, Mishra A (2020) Applications of paper as a support material in biomedical sciences: a decadal review. *SI: 100004*. <https://doi.org/10.1016/j.sintl.2020.100004>
- Derda R, Tang SK, Laromaine A, Mosadegh B, Hong E, Mwangi M, Mammoto A, Ingber DE, Whitesides GM (2011) Multizone paper platform for 3D cell cultures. *PLoS ONE* 6(5):e18940. <https://doi.org/10.1371/journal.pone.0018940>
- Dudte LH, Vouga E, Tachi T, Mahadevan L (2016) Programming curvature using origami tessellations. *Nat Mater* 15(5):583–588
- Eslami M, Vrana NE, Zorlutuna P, Sant S, Jung S, Masoumi N, Khavari-Nejad RA, Javadi G, Khademhosseini A (2014) Fiber-reinforced hydrogel scaffolds for heart valve tissue engineering. *J Biomater Appl* 29(3):399–410. <https://doi.org/10.1177/0885328214530589>
- Hidalgo-Bastida L, Barry J, Everitt N, Rose F, BATTERY L, Hall I, Claycomb W, Shakesheff K (2007) Cell adhesion and mechanical properties of a flexible scaffold for cardiac tissue engineering. *Acta Biomater* 3(4):457–462. <https://doi.org/10.1016/j.actbio.2006.12.006>
- Juvonen H, Maattanen A, Lauren P, Ihalainen P, Urtti A, Yliperttula M, Peltonen J (2013) Biocompatibility of printed paper-based arrays for 2-D cell cultures. *Acta Biomater* 9(5):6704–6710. <https://doi.org/10.1016/j.actbio.2013.01.033>
- Kai D, Prabhakaran MP, Jin G, Ramakrishna S (2011) Guided orientation of cardiomyocytes on electrospun aligned nanofibers for cardiac tissue engineering. *J Biomed* 98(2):379–386. <https://doi.org/10.1002/jbm.b.31862>
- Kapnisi M, Mansfield C, Marijon C, Guex AG, Perbellini F, Bardi I, Humphrey EJ, Puetzer JL, Mawad D, Koutsogeorgis DC (2018) Auxetic cardiac patches with tunable mechanical and conductive properties toward treating myocardial infarction. *Adv Funct Mater* 28(21):1800618. <https://doi.org/10.1002/adfm.201800618>

- Ker ED, Nain AS, Weiss LE, Wang J, Suhan J, Amon CH, Campbell PG (2011) Bioprinting of growth factors onto aligned sub-micron fibrous scaffolds for simultaneous control of cell differentiation and alignment. *Biomaterials* 32(32):8097–8107. <https://doi.org/10.1016/j.biomaterials.2011.07.025>
- Khan M, Xu Y, Hua S, Johnson J, Belevych A, Janssen PM, Gyorke S, Guan J, Angelos MG (2015) Evaluation of changes in morphology and function of human induced pluripotent stem cell derived cardiomyocytes (HiPSC-CMs) cultured on an aligned-nanofiber cardiac patch. *PLoS ONE* 10(5):e0126338. <https://doi.org/10.1371/journal.pone.0126338>
- Kharaziha M, Nikkha M, Shin S-R, Annabi N, Masoumi N, Gaharwar AK, Camci-Unal G, Khademhosseini A (2013) PGS: gelatin nanofibrous scaffolds with tunable mechanical and structural properties for engineering cardiac tissues. *Biomaterials* 34(27):6355–6366. <https://doi.org/10.1016/j.biomaterials.2013.04.045>
- Kim Y, Son K, Lee J (2021) Auxetic structures for tissue engineering scaffolds and biomedical devices. *Materials* 14(22):6821. <https://doi.org/10.3390/ma14226821>
- Kröling H, Endres A, Nubbo N, Fleckenstein J, Miletzky A, Schabel S (2014) Anisotropy of paper and paper based composites and the modelling thereof. *ECCM* 16:1–8
- Kuribayashi K, Tsuchiya K, You Z, Tomus D, Umemoto M, Ito T, Sasaki M (2006) Self-deployable origami stent grafts as a biomedical application of Ni-rich TiNi shape memory alloy foil. *Mater Sci Eng A* 419(1–2):131–137. <https://doi.org/10.1016/j.msea.2005.12.016>
- Lantigua D, Kelly YN, Unal B, Camci-Unal G (2017) Engineered paper-based cell culture platforms. *Adv Healthc Mater* 6(22):1700619. <https://doi.org/10.1002/adhm.201700619>
- Li H, Cheng F, Robledo-Lara JA, Liao J, Wang Z, Zhang YS (2020) Fabrication of paper-based devices for in vitro tissue modeling. *Bio-Des Manuf* 3:252–265. <https://doi.org/10.1007/s42242-020-00077-5>
- Li S, Vogt DM, Rus D, Wood RJ (2017) Fluid-driven origami-inspired artificial muscles. *Proc Natl Acad Sci* 114(50):13132–13137. <https://doi.org/10.1073/pnas.1713450114>
- Miura K (1985) Method of packaging and deployment of large membranes in space. *Inst Space Astronaut Sci Rep* 618:1–9
- Moroni L, Burdick JA, Highley C, Lee SJ, Morimoto Y, Takeuchi S, Yoo JJ (2018) Biofabrication strategies for 3D in vitro models and regenerative medicine. *Nat Rev Mater* 3(5):21–37. <https://doi.org/10.1038/s41578-018-0006-y>
- Mosadegh B, Dabiri BE, Lockett MR, Derda R, Campbell P, Parker KK, Whitesides GM (2014) Three-dimensional paper-based model for cardiac ischemia. *Adv Healthc Mater* 3(7):1036–1043. <https://doi.org/10.1002/adhm.201300575>
- Mosadegh B, Lockett MR, Minn KT, Simon KA, Gilbert K, Hillier S, Newsome D, Li H, Hall AB, Boucher DM (2015) A paper-based invasion assay: assessing chemotaxis of cancer cells in gradients of oxygen. *Biomaterials* 52:262–271. <https://doi.org/10.1016/j.biomaterials.2015.02.012>
- Müller FA, Müller L, Hofmann I, Greil P, Wenzel MM, Staudenmaier R (2006) Cellulose-based scaffold materials for cartilage tissue engineering. *Biomaterials* 27(21):3955–3963. <https://doi.org/10.1016/j.biomaterials.2006.02.031>
- Ng K, Gao B, Yong KW, Li Y, Shi M, Zhao X, Li Z, Zhang X, Pinguang-Murphy B, Yang H, Xu F (2017) Paper-based cell culture platform and its emerging biomedical applications. *Mater Today* 20(1):32–44. <https://doi.org/10.1016/j.mattod.2016.07.001>
- Park HJ, Yu SJ, Yang K, Jin Y, Cho AN, Kim J, Lee B, Yang HS, Im SG, Cho SW (2014) Paper-based bioactive scaffolds for stem cell-mediated bone tissue engineering. *Biomaterials* 35(37):9811–9823. <https://doi.org/10.1016/j.biomaterials.2014.09.002>
- Parnell V (2021) Self-folding Non-Invasive Miniature Robots: Progress and Trend in the Biomedical Field. *Nano Biomed Eng.* <https://doi.org/10.5101/nbe.v13i4.p329-343>
- Parrag IC, Zandstra PW, Woodhouse KA (2012) Fiber alignment and coculture with fibroblasts improves the differentiated phenotype of murine embryonic stem cell-derived cardiomyocytes for cardiac tissue engineering. *Biotechnol Bioeng* 109(3):813–822. <https://doi.org/10.1002/bit.23353>
- Philpott R (2012) Crafting innovation: the intersection of craft and technology in the production of contemporary textiles. *Craft Res* 3(1):53–74. https://doi.org/10.1386/crrc.3.1.53_1
- Pushp P, Bhaskar R, Kelkar S, Sharma N, Pathak D, Gupta MK (2021) Plasticized poly (vinylalcohol) and poly (vinylpyrrolidone) based patches with tunable mechanical properties for cardiac tissue engineering applications. *Biotechnol Bioeng* 118(6):2312–2325. <https://doi.org/10.1002/bit.27743>
- Radisic M, Park H, Shing H, Consi T, Schoen FJ, Langer R, Freed LE, Vunjak-Novakovic G (2004) Functional assembly of engineered myocardium by electrical stimulation of cardiac myocytes cultured on scaffolds. *Proc Natl Acad Sci* 101(52):18129–18134. <https://doi.org/10.1073/pnas.0407817101>
- Rayatpisheh S, Heath DE, Shakouri A, Rujitanaroj P-O, Chew SY, Chan-Park MB (2014) Combining cell sheet technology and electrospun scaffolding for engineered tubular, aligned, and contractile blood vessels. *Biomaterials* 35(9):2713–2719. <https://doi.org/10.1016/j.biomaterials.2013.12.035>
- Reid A, Lechenault F, Rica S, Adda-Bedia M (2017) Geometry and design of origami bellows with tunable response. *Phys Rev E* 95(1):013002. <https://doi.org/10.1103/PhysRevE.95.013002>
- Rodrigues GV, Fonseca LM, Savi MA, Paiva A (2017) Non-linear dynamics of an adaptive origami-stent system. *Int J Mech Sci* 133:303–318. <https://doi.org/10.1016/j.ijmecsci.2017.08.050>
- Schenk M, Allwood J, Guest S (2011) Cold gas-pressure folding of Miura-ori sheets. In: *Steel research international, special issue proceedings of the international conference on technology of plasticity (ICTP)*
- Schenk M, Guest SD (2013) Geometry of Miura-folded metamaterials. *Proc Natl Acad Sci* 110(9):3276–3281. <https://doi.org/10.1073/pnas.1217998110>

- Tsai C-Y, Lin C-L, Cheng N-C, Yu J (2017) Effects of nano-grooved gelatin films on neural induction of human adipose-derived stem cells. *RSC Adv* 7(84):53537–53544. <https://doi.org/10.1039/C7RA09020J>
- Tseng L-F, Mather PT, Henderson JH (2013) Shape-memory-actuated change in scaffold fiber alignment directs stem cell morphology. *Acta Biomater* 9(11):8790–8801. <https://doi.org/10.1016/j.actbio.2013.06.043>
- Wang L, Xu C, Zhu Y, Yu Y, Sun N, Zhang X, Feng K, Qin J (2015) Human induced pluripotent stem cell-derived beating cardiac tissues on paper. *Lab Chip* 15(22):4283–4290. <https://doi.org/10.1039/c5lc00919g>
- Wanjare M, Hou L, Nakayama KH, Kim JJ, Mezak NP, Abilez OJ, Tzatzalos E, Wu JC, Huang NF (2017) Anisotropic microfibrous scaffolds enhance the organization and function of cardiomyocytes derived from induced pluripotent stem cells. *Biomater Sci* 5(8):1567–1578. <https://doi.org/10.1039/c7bm00323d>
- Whited BM, Rylander MN (2014) The influence of electro-spun scaffold topography on endothelial cell morphology, alignment, and adhesion in response to fluid flow. *Biotechnol Bioeng* 111(1):184–195. <https://doi.org/10.1002/bit.24995>
- Wohlert M, Bensselfelt T, Wågberg L, Furó I, Berglund LA, Wohlert J (2021) Cellulose and the role of hydrogen bonds: not in charge of everything. *Cellulose* 29:1–23. <https://doi.org/10.1007/s10570-021-04325-4>
- Woodruff SR, Filipov ET (2021) Curved creases redistribute global bending stiffness in corrugations: theory and experimentation. *Meccanica* 56(6):1613–1634. <https://doi.org/10.1007/s11012-020-01200-7>
- Woodruff SR, Filipov ET (2022) Bending and twisting with a pinch: shape morphing of creased sheets. *Extreme Mech Lett* 52:101656. <https://doi.org/10.1016/j.eml.2022.101656>

Publisher's Note Springer Nature remains neutral with regard to jurisdictional claims in published maps and institutional affiliations.